

## PHYSICS

# Observation of new plasmons in the fractional quantum Hall effect: Interplay of topological and nematic orders

Lingjie Du<sup>1\*</sup>, Ursula Wurstbauer<sup>2,3</sup>, Ken W. West<sup>4</sup>, Loren N. Pfeiffer<sup>4</sup>, Saeed Fallahi<sup>5,6</sup>, Geoff C. Gardner<sup>6,7</sup>, Michael J. Manfra<sup>5,6,7,8</sup>, Aron Pinczuk<sup>1,9</sup>

Collective modes of exotic quantum fluids reveal underlying physical mechanisms responsible for emergent quantum states. We observe unexpected new collective modes in the fractional quantum Hall (FQH) regime: intra-Landau-level plasmons measured by resonant inelastic light scattering. The plasmons herald rotational-symmetry-breaking (nematic) phases in the second Landau level and uncover the nature of long-range translational invariance in these phases. The intricate dependence of plasmon features on filling factor provides insights on interplays between topological quantum Hall order and nematic electronic liquid crystal phases. A marked intensity minimum in the plasmon spectrum at Landau level filling factor  $\nu = 5/2$  strongly suggests that this paired state, which may support non-Abelian excitations, overwhelms competing nematic phases, unveiling the robustness of the  $5/2$  superfluid state for small tilt angles. At  $\nu = 7/3$ , a sharp and strong plasmon peak that links to emerging macroscopic coherence supports the proposed model of a FQH nematic state.

## INTRODUCTION

The interplay between quantum electronic liquid crystal (QELC) phases and quantum liquids is a key topic of condensed matter physics that is intensely studied in two-dimensional (2D) systems (1–14) and in high-temperature superconductors (2, 15, 16). In partially filled Landau levels (LLs) of 2D electron gases, early theoretical work based on the Hartree-Fock approximation suggested the presence of unidirectional charge density wave (CDW) order that is a precursor of QELC phases (1, 7). When quantum and thermal fluctuations were considered (2, 3, 8), understanding of the CDW progressed and uncovered several possibilities of QELC phases (including nematic phases, smectic phases, and stripe crystal). In candidate QELC phases that break full rotational symmetry, the nematic phases are the ones that have full translational invariance at long ranges, the smectic phases break translational symmetry in one spatial direction (perpendicular to stripe-like structures), and the stripe crystal phases break translational symmetry.

In the partially filled second LL (SLL), the broken rotational symmetry phases induced under in-plane magnetic fields, which interplay with quantum Hall fluids (topological order), were mainly studied by anisotropic transport experiments (4, 6, 17–19) and spin-wave excitations (20–22). The quantum Hall fluids in the SLL include the enigmatic even-denominator fractional quantum Hall (FQH) state at  $\nu = 5/2$ , described as a p-wave paired superfluid phase (23–26), and new unconventional odd-denominator FQH states. At  $\nu = 7/3$ , the application of even small in-plane magnetic fields caused a marked transport anisotropy that coexisted with the quantized Hall plateau (17). The results indicate the formation of emerging QELC phases that are closely linked to FQH edge states, leading to interpretations in terms of a new state of electron matter

with FQH states that occur in the environment of a nematic phase (FQH nematic phase) (9–12, 14, 27, 28). Recently, anisotropic transport with isotropic activation energies reported at  $\nu = 5/2$  was interpreted as the formation of a FQH nematic phase (19). On the other hand, a compressible nematic phase could occur at  $\nu = 5/2$ , which took over the  $5/2$  FQH state at sufficiently large in-plane magnetic fields (4, 6, 18, 29, 30). Although properties of broken rotational invariance were intensively studied in these phases, long-range translational invariance has not been accessed. Experimentally probing the simultaneous emergence of broken rotational symmetry and long-range translational symmetry (especially along the spatial direction perpendicular to stripe-like structures) is important to identify the nematic order.

## RESULTS AND DISCUSSION

Here, we report the observation of new collective modes in the partially populated SLL in tilted magnetic fields. The experiments are carried out in systems where measurements of long-wavelength spin-wave excitations demonstrate broken rotational invariance that may be associated with anisotropic transport (20–22). The new collective modes are identified as plasmon-like excitations from nematic phases that occur in the filling factor range of  $2 < \nu < 3$  of the SLL. Observed plasmon energies are well below the cyclotron energy, showing that the modes are intra-LL plasmons. To the best of our knowledge, these collective modes have not been reported or considered in quantum Hall systems. It is notable that intra-LL plasmon modes are observed at specific filling factors of FQH states and at non-FQH filling factors. The observed wave vector dependence of the mode energy reveals full translational invariance in QELC phases for mode wavelengths much longer than the magnetic length. The observations offer new insights on the interplay between nematic and FQH orders that can now be directly probed in the bulk, without the intermediacy of edge states that occurs in transport.

The intra-LL plasmons in the SLL are observed by resonant inelastic light scattering (RILS) methods. The measured collective mode energy is described by

$$\omega(q) = (1 + \xi)\omega_p(q) \quad (1)$$

<sup>1</sup>Department of Applied Physics and Applied Mathematics, Columbia University, New York, NY 10027, USA. <sup>2</sup>Walter Schottky Institut and Physik-Department, Technische Universität München, Am Coulombwall 4a, 85748 Garching, Germany. <sup>3</sup>Institute of Physics, University of Münster, Wilhelm-Klemm-Str.10, 48149 Münster, Germany. <sup>4</sup>Department of Electrical Engineering, Princeton University, Princeton, NJ 08544, USA. <sup>5</sup>Department of Physics and Astronomy, Purdue University, IN 47907, USA. <sup>6</sup>Birck Nanotechnology Center, Purdue University, IN 47907, USA. <sup>7</sup>Microsoft Station Q Purdue, Purdue University, IN 47907, USA. <sup>8</sup>School of Materials Engineering and School of Electrical and Computer Engineering, IN 47907, USA. <sup>9</sup>Department of Physics, Columbia University, New York, NY 10027, USA.

\*Corresponding author. Email: ld2751@columbia.edu

where  $\xi \ll 1$  is a dimensionless parameter and  $\omega_p(q)$  is the plasmon energy of a 2D electron system that has full translational symmetry (31)

$$\omega_p = \sqrt{n^* e^2 q / (2\epsilon\epsilon_0 m^*)} \quad (2)$$

where  $q = k$ , and  $k$  is the wave vector transferred in light scattering experiments (see Materials and Methods).  $m^*$  is the band mass of electrons in the GaAs quantum well.  $\epsilon$  and  $\epsilon_0$  are the background dielectric constant and free-space permittivity, respectively. The parameter  $n^*$  is a quasiparticle density in the spin-up SLL, which depends on magnetic fields. The interpretation in terms of the plasmon energy of an electron system with full translational symmetry suggests that the plasmon wave vector  $q$  is largely a good quantum number for wavelengths  $\lambda_{ij} = 2\pi/q$ , much larger than characteristic periods in QELC phases. Then, the QELC phases that support the observed intra-LL plasmons recover long-range translational invariance at the wave vector and temperature accessible in this experiment. Given that nematics are the QELC phases that have translational invariance, the modes described by Eqs. 1 and 2 are intra-LL plasmons in nematic phases in the partially populated SLL.

The observation of these intra-LL plasmons is fully unexpected and demonstrates a new venue to explore exotic quantum liquids in quantum Hall systems. At  $\nu = 5/2$ , the intensity of the plasmon line in the SLL is found to have a marked minimum. This observation suggests that an even-denominator FQHE state at  $\nu = 5/2$  overwhelms the nematic phase. The  $5/2$  state is currently understood as a gapped state of paired composite fermions. The minimum in the plasmon intensity suggests a suppression of the nematic phase that could be due to the tendency of a superfluid phase to extend to the whole 2D electron system. The robustness of the  $5/2$  state could be crucial in potential applications of the state in topological quantum computation (26).

Quite unexpectedly, as we approach the filling factor  $\nu = 7/3$ , the intensity of a very sharp plasmon line is strongly enhanced. This un-

anticipated enhancement indicates that, as topological FQH order appears at  $\nu = 7/3$ , there is no competition with the nematic order, but rather, that topological order and the nematic order coexist at  $\nu = 7/3$ . This observation is regarded as direct evidence for the proposed frameworks of nematic FQH states (9–12, 14, 27, 28) and represents the application of an incisive experimental probe to the study of a novel quantum many-body phase that simultaneously displays both topological order and broken geometric symmetries.

An ultraclean 2D electron system that enables RILS observations of several gapped FQHE states and spin-wave excitations in the SLL (20–22) is used in our measurements in the backscattering geometry setup shown in Fig. 1A (details can be found in Materials and Methods). Figure 1B illustrates RILS spectra at filling factor  $\nu = 7/3$ , showing the resonance-enhanced mode at 1.43 meV. Similar modes exist in both FQH and non-FQH states, at energies that depend on filling factor in the range of  $2 < \nu < 3$ , as shown in Fig. 1C. Nevertheless, the mode is absent at filling factor  $\nu = 2$  and 3. The mode energies are significantly higher than those of neutral gap excitations of FQH states and of spin-wave excitations in the SLL (20–22) but are much lower than those of inter-LL magnetoplasmons (32).

To understand the mode in the partially populated SLL, we use the quasiparticle density  $n^*$  that is equal to the degrees of freedom for intra-LL transitions (from occupied to empty states in the same LL). For  $\nu < 5/2$ ,  $n^*$  is given by the electron density in the partially populated SLL  $n_e = n - 2eB_{\perp}/h$ , where  $B_{\perp}$  is the perpendicular magnetic field and  $h$  is the Planck constant. For  $\nu > 5/2$ , the Pauli exclusion principle limits the degrees of freedom to the density of holes (empty states in the SLL) given by  $n_h = 3eB_{\perp}/h - n$ . Figure 2A reports that, for  $2 < \nu \leq 5/2$ , the plasmon energy is proportional to the square root of  $n_e$ , and, for  $5/2 \leq \nu < 3$ , the energy is proportional to the square root of  $n_h$ . Figure 2B displays the mode energies in a single plot, revealing a slight difference between plasmons linked to  $n_e$  and  $n_h$ . Well-defined plasmon energies suggest wave vector conservation  $q = k$  in RILS experiments. We fit the square-root dependences using Eqs. 1 and 2 with  $k = 5.3 \times 10^4 \text{ cm}^{-1}$ ,

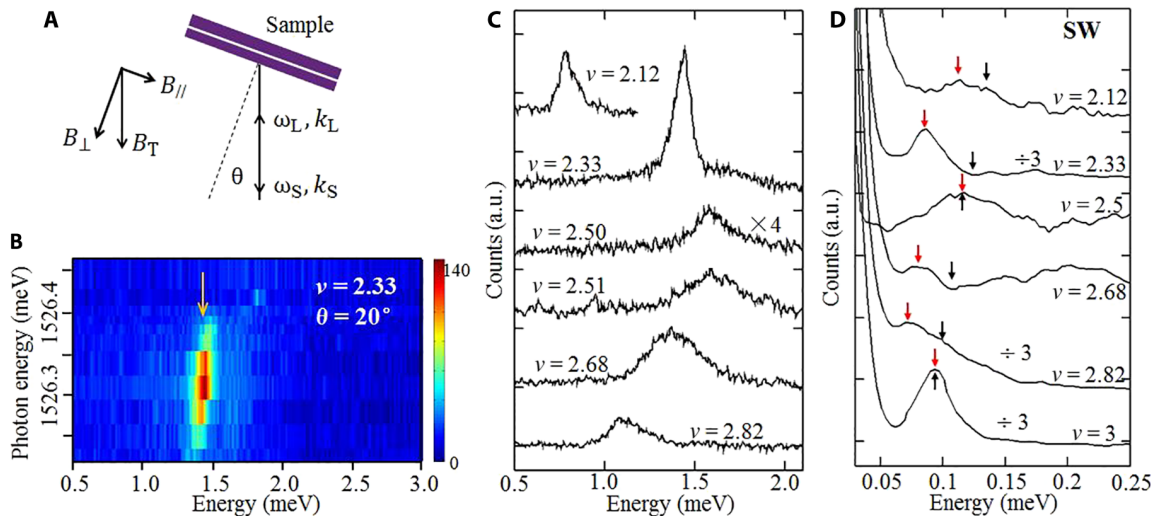


**Fig. 1. Observation of new plasmons in the SLL.** (A) Schematic description of the light scattering geometry at a tilt angle  $\theta$ . Incident and scattered light have photon energy  $\omega_L$  and  $\omega_S$  and wave vector  $k_L$  and  $k_S$ . The total magnetic field  $B_T$ , the perpendicular component  $B_{\perp}$ , and in-plane magnetic field  $B_{\parallel}$  are also shown.  $k = 5.3 \times 10^4 \text{ cm}^{-1}$  for  $\theta = 20^\circ$  and  $\omega_L = 1526 \text{ meV}$ . (B) Color plot of RILS spectra of the plasmon measured at  $\theta = 20^\circ$  in the QELC phase at  $\nu = 2.33$  as a function of  $\omega_L$ . The mode intensity is resonantly enhanced at the plasmon energy (1.43 meV) marked by an arrow. (C) RILS spectra of plasmons at filling factors in the range  $2 < \nu < 3$ . Intensities of the spectra in (B) and (C) are normalized to the incident light intensity. (D) Spin-wave (SW) modes in the range of  $2 < \nu \leq 3$ . Red arrows mark the position of the spin-wave modes, and black arrows indicate the Zeeman energy. a.u., arbitrary units.

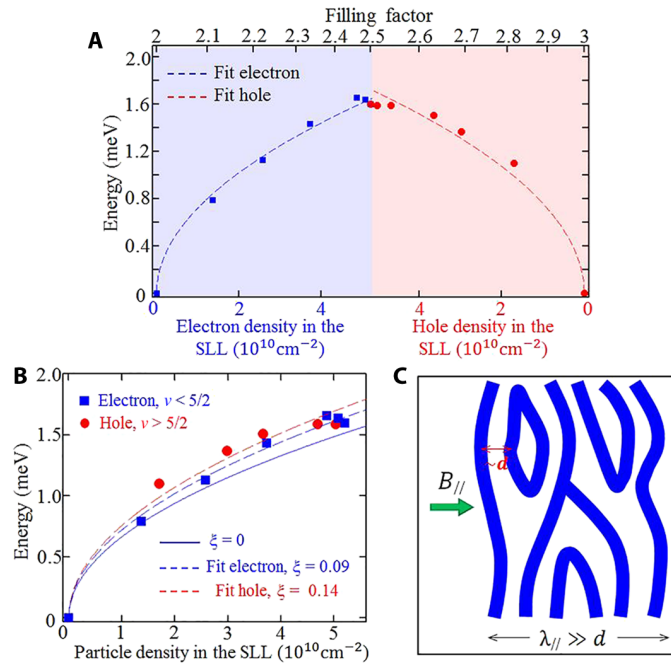


**Fig. 2. Square-root dependence of plasmon energy on particle density.** (A) Plasmon energy as a function of particle density in the filling factor range of the spin-up SLL. The blue squares are for electrons, and the red dots are for holes. The blue dashed line is a fit with a square-root dependence on electron density, and the red dashed line is a fit with a square-root dependence on hole density. (B) Data points in (A) as a function of particle density  $n^*$ . The square-root dependence is described by Eq. 1, where  $m^* = 0.07 m_0$ ,  $q = 5.3 \times 10^4 \text{ cm}^{-1}$ ,  $\epsilon = (\epsilon_{\text{GaAs}} + \epsilon_{\text{AlGaAs}})/2 = 12.5$ ,  $\epsilon_{\text{GaAs}}$  is the dielectric constant of GaAs,  $\epsilon_{\text{AlGaAs}}$  is the dielectric constant of AlGaAs,  $\alpha = 0.09$  for electrons, and  $\alpha = 0.14$  for holes. (C) Cartoon showing charge stripes in the SLL under an in-plane magnetic field. For the wave vector  $q \parallel B_{||}$  (see Fig. 1A), the plasmon wavelength  $\lambda_{||} = 2\pi/q$  is much larger than a typical spacing between stripes (a few magnetic lengths).

the value of  $k$  at tilt angle  $\theta = 20^\circ$ , and  $m^* = 0.07 m_0$ , the band mass of electrons in GaAs. We treat  $\xi$  as an adjustable parameter. The best fits shown in Fig. 2B as dashed lines are achieved with  $\xi = 0.09$  for  $\nu \leq 5/2$  and  $\xi = 0.14$  for  $\nu > 5/2$ . In fig. S1, we plot the mode energy versus density on a log-log plot. In these data, the density dependence of the mode energy is dominated by a square root. Slight departures from the square-root dependence are attributed to the small uncertainty of the determination of plasmon energy. Equations 1 and 2 are a phenomenological description of the data. A model of the dielectric function of the nematic states could eventually predict values of the parameter  $\xi$ .

Under in-plane magnetic fields, broken rotational invariance in emergent QELC phases in the partially populated SLL is demonstrated in RILS measurements of long-wavelength spin-wave excitations shown in Fig. 1D. At  $\nu = 3$ , the electron system in the SLL has full in-plane rotational invariance, and the spin wave occurs at the bare Zeeman energy as required by Larmor's theorem (20–22, 33). As the plasmon modes appear for  $\nu < 3$ , the spin-wave modes soften with the departure of the spin-wave peaks from the bare Zeeman energy, which breaks Larmor's theorem at long-wavelength limit and demonstrates the broken rotational invariance of emergent nematic QELC phases. In samples, because of the broken rotational symmetry, locally stripe-like structures would form. As sketched in Fig. 2C, the transferred wave vector  $k \parallel B_{||}$  is perpendicular to stripe-like structures in QELC phases (4, 6). A typical spacing between stripes  $d$  is understood to be on a length scale of a few magnetic lengths  $l \approx 11 \text{ nm}$  (1, 7, 30), which is much shorter than the plasmon wavelength  $\lambda_{||} = 2\pi/k = 1.18 \mu\text{m}$ . Thus, plasmon excitations have a long wavelength, with the local nonuniform charge density in QELC phases not resolved. The determined parameter

$\xi \ll 1$  suggests that the measured points are described by a plasmon equation with a small plasmon wave vector  $q = k$ . For this reason,  $q$  is a good quantum number in the long-wavelength limit ( $\lambda_{||} \gg d$ ), revealing the long-range translational invariance in the QELC phase. Thus, in our experiments, probing the simultaneous emergence of broken rotational symmetry and full translational invariance identifies the presence of the nematic order.

The observations of plasmon modes of nematic phases offer direct insights on interplays of nematic order and the topological order in FQH liquids. Figure 3A shows normalized integrated intensities  $I^* = I/n^*$ , where  $I$  is the integrated intensity of the plasmon peak,  $n^* = n_e$  for  $\nu < 5/2$  and  $n^* = n_h$  for  $\nu > 5/2$ . The measured values of  $I^*$  are close to 3 at filling factors away from FQH states. Unexpectedly, at the  $\nu = 7/3$  FQH state,  $I^*$  increases by about a factor of two. This is a significant result that indicates a remarkable link between the nematic phase and the FQH state at  $\nu = 7/3$ . We consider a model of plasmons in nematics in which the mode wave vector  $q$  has real and imaginary parts  $\text{Re } q$  and  $\text{Im } q$ . Wave vector conservation in RILS means that  $k = \text{Re } q$ . A nonzero value of  $\text{Im } q$  brings a finite plasmon coherence length  $L = 2\pi/\text{Im } q$ , which results in a small breakdown of the wave vector conservation selection rule in the light scattering process (34). As a result, RILS occurs in modes with a range  $\Delta q = \text{Im } q = 2\pi/L$ . In this model, the maximum RILS intensity of the plasmon line is proportional to  $1/\Delta q^2 \propto L^2$ . Thus, the enhanced plasmon intensity at  $\nu = 7/3$  demonstrates an enhanced value of  $L$  as the FQH state at  $\nu = 7/3$  is reached. The breakdown of exact wave vector conservation in RILS would result in a full width at half maximum (FWHM)  $\Delta\omega = \omega(q)\Delta q/q$  of the plasmon line that is used to estimate  $L$ . Figure 3B shows that, at  $\nu = 7/3$ , the length  $L$  reaches its maximum value. These results could be linked to macroscopic coherence

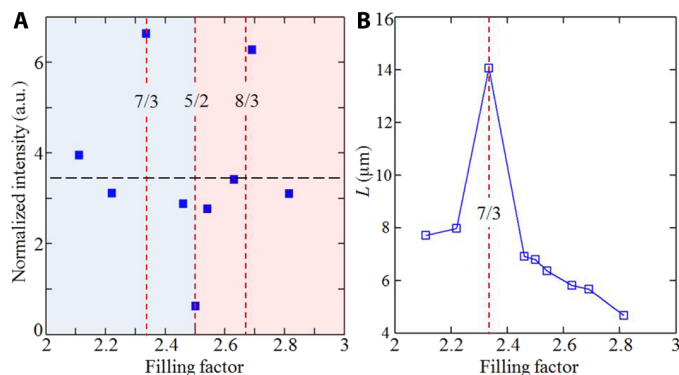


**Fig. 3. Dependence of plasmon intensity on filling factor.** (A) Normalized integrated intensity of the plasmon peaks as a function of filling factor. The integrated intensity is normalized by particle density in the SLL. The black dashed line marks a background value of electronic liquid crystal phases in the SLL. Three red dashed lines mark filling factors of  $\nu = 7/3$ ,  $5/2$ , and  $8/3$  respectively. (B) Characteristic plasmon coherence length  $L$  as a function of filling factor.  $L$  is determined from the FWHM of the plasmon lines.

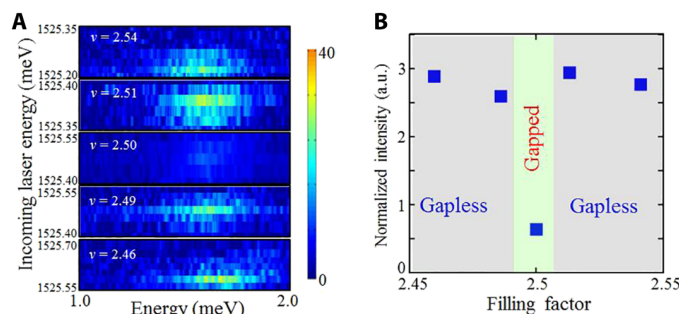


**Fig. 4. Plasmon modes near  $\nu = 5/2$ .** (A) Color plots of RILS spectra measured at filling factors around  $\nu = 2.50$  as function of incoming photon energy  $\omega_L$ . Resonance of the plasmon modes appears at close  $\omega_L$  for filling factors around  $\nu = 5/2$ . (B) Normalized integrated intensity of the plasmon peaks around  $\nu = 2.50$ . The green area indicates the appearance of the gapped (incompressible) FQH state, while the gray area indicates gapless (compressible) FQH states (20).

in FQH nematics when the emergent topological FQH order has long-range correlations that favor translational invariance. We are thus led to propose that the dependence of plasmon intensity and lineshape in RILS spectra displayed in Fig. 3 gives crucial support to FQH nematic frameworks that describe the states near  $\nu = 7/3$ . Figure 3A also shows a plasmon intensity maximum at a filling factor close to  $\nu = 8/3$ , the particle-hole conjugate state of the  $7/3$  state, indicating a possible nematic presence in the FQH phase at  $\nu = 8/3$ . The smaller  $L$  (larger  $\Delta\omega$ ) for  $\nu > 5/2$  indicates that hole-like plasmon excitations are more sensitive to disorder.

Figure 3B shows that there is continuity in the plasmon coherence length for filling factors in the vicinity of  $\nu = 5/2$ , which suggests that the plasmon mode at  $\nu = 5/2$  is from a phase similar to that at non-FQH states, i.e., a compressible nematic phase, not the  $5/2$  FQH state. Figure 3A shows that, at  $\nu = 5/2$ , the normalized integrated plasmon intensity collapses by nearly 80% from the intensity at non-FQH states (shown by the black dashed line in Fig. 3A). As illustrated in Fig. 4 (A and B), the plasmon intensity recovers for small changes  $|\Delta\nu| \leq 0.01$  away from  $\nu = 5/2$ . The sudden drop of the plasmon intensity suggests that the nematic order is replaced by the FQH topological order in a quantum phase transition at  $\nu = 5/2$ . In other words, the incompressible  $5/2$  state, proposed as the superfluid of paired composite fermions, dominates over the competing nematic phase. This interpretation is consistent with the recovery of rotational invariance manifested in the appearance of long-wavelength spin waves at the Zeeman energy, as shown in Fig. 1D for  $\nu = 5/2$ . The collapsing plasmon intensity confirms that the gapped

$5/2$  state does not support a plasmon mode described by Eq. 1. The distinct behaviors of the plasmon modes at  $\nu = 5/2$  and  $7/3$  here reveal that the robust  $5/2$  state suppresses the nematic phase, while the  $7/3$  state has a phase transition to the nematic FQH state.

In conclusion, observations of new intra-Landau-level plasmon modes of nematic phases indicate the complex interplay between topological order and symmetry-breaking phases of 2D electron systems. The sharp and intense plasmon peak in the state at  $\nu = 7/3$  reveals that the macroscopic coherence of the FQH liquid coexists with nematic order, which is a key signature of a FQH nematic phase. In contrast, the collapse of the plasmon mode intensity at  $\nu = 5/2$  uncovers that the robust gapped superfluid phase competes with and takes over the nematic phase.

## MATERIALS AND METHODS

The ultraclean 2D electron system is confined in a 30-nm-wide, double-sided, modulation-doped GaAs/AlGaAs quantum well. The electron density is  $n = 2.9 \times 10^{15} \text{ m}^{-2}$ , and the mobility is  $\mu = 23.9 \times 10^2 \text{ m}^2/\text{Vs}$  at 300 mK. The high sample quality enables RILS observations of several gapped FQHE states in the SLL (20–22). The backscattering geometry described in Fig. 1A was used in optics measurements with a small tilt angle  $\theta \approx 20^\circ$  in a dilution refrigerator operating at a base temperature below 40 mK. In RILS, there is a finite wave vector transfer  $k = |k_L - k_S| \sin\theta = (2\omega_L/c) \sin\theta = 5.3 \times 10^6 \text{ m}^{-1}$ , where  $k_L$  and  $k_S$  are wave vectors of the incident and scattered photons,  $\omega_L$  is the incident



photon energy, and  $c$  is the speed of light in vacuum. In our experiments, the wave vector  $k$  that is transferred in light scattering experiments is much smaller than  $1/l$  ( $l$  is the magnetic length), suggesting that  $k$  is in the long-wavelength limit. As shown in Fig. 1A, the back-scattering geometry allows in-plane components of applied magnetic fields. Since the incident/scattered light is parallel to the total magnetic fields, the transferred wave vectors in light scattering are parallel to the in-plane magnetic fields.

## SUPPLEMENTARY MATERIALS

Supplementary material for this article is available at <http://advances.sciencemag.org/cgi/content/full/5/3/eaav3407/DC1>

Fig. S1. The plasmon energy versus particle density  $n^*$  on a log-log plot.

## REFERENCES AND NOTES

- M. M. Fogler, A. A. Koulakov, B. I. Shklovskii, Ground state of a two-dimensional electron liquid in a weak magnetic field. *Phys. Rev. B* **54**, 1853–1871 (1996).
- S. A. Kivelson, E. Fradkin, V. J. Emery, Electronic liquid-crystal phases of a doped Mott insulator. *Nature* **393**, 550–553 (1998).
- E. Fradkin, S. A. Kivelson, Liquid-crystal phases of quantum Hall systems. *Phys. Rev. B* **59**, 8065–8072 (1999).
- M. P. Lilly, K. B. Cooper, J. P. Eisenstein, L. N. Pfeiffer, K. W. West, Evidence for an anisotropic state of two-dimensional electrons in high Landau levels. *Phys. Rev. Lett.* **82**, 394–397 (1999).
- R. R. Du, D. C. Tsui, H. L. Stormer, L. N. Pfeiffer, K. W. Baldwin, K. W. West, Strongly anisotropic transport in higher two-dimensional Landau levels. *Solid State Commun.* **109**, 389–394 (1999).
- W. Pan, R. R. Du, H. L. Stormer, D. C. Tsui, L. N. Pfeiffer, K. W. Baldwin, K. W. West, Strongly anisotropic electronic transport at Landau level filling factor  $\nu = 9/2$  and  $\nu = 5/2$  under a tilted magnetic field. *Phys. Rev. Lett.* **83**, 820–823 (1999).
- R. Moessner, J. T. Chalker, Exact results for interacting electrons in high Landau levels. *Phys. Rev. B* **54**, 5006–5015 (1996).
- E. Fradkin, S. A. Kivelson, M. J. Lawler, J. P. Eisenstein, A. P. Mackenzie, Nematic Fermi fluids in condensed matter physics. *Annu. Rev. Condens. Matter Phys.* **1**, 153–178 (2010).
- M. Mulligan, C. Nayak, S. Kachru, Isotropic to anisotropic transition in a fractional quantum Hall state. *Phys. Rev. B* **82**, 085102 (2010).
- M. Mulligan, C. Nayak, S. Kachru, Effective field theory of fractional quantized Hall nematics. *Phys. Rev. B* **84**, 195124 (2011).
- J. Maciejko, B. Hsu, S. A. Kivelson, Y. Park, S. L. Sondhi, Field theory of the quantum Hall nematic transition. *Phys. Rev. B* **88**, 125137 (2013).
- Y. You, G. Y. Cho, E. Fradkin, Theory of Nematic Fractional Quantum Hall States. *Phys. Rev. X* **4**, 041050 (2014).
- Q. Qian, J. Nakamura, S. Fallahi, G. C. Gardner, M. J. Manfra, Possible nematic to smectic phase transition in a two-dimensional electron gas at half-filling. *Nat. Commun.* **8**, 1536 (2017).
- A. Gromov, D. T. Son, Bimetric Theory of Fractional Quantum Hall States. *Phys. Rev. X* **7**, 041032 (2017).
- J. M. Tranquada, B. J. Sternlieb, J. D. Axe, Y. Nakamura, S. Uchida, Evidence for stripe correlations of spins and holes in copper oxide superconductors. *Nature* **375**, 561–563 (1995).
- V. Hinkov, D. Haug, B. Fauqué, P. Bourges, Y. Sidis, A. Ivanov, C. Bernhard, C. T. Lin, B. Keimer, Electronic liquid crystal state in the high-temperature superconductor  $\text{YBa}_2\text{Cu}_3\text{O}_{6.45}$ . *Science* **319**, 597–600 (2008).
- J. Xia, J. P. Eisenstein, L. N. Pfeiffer, K. W. West, Evidence for a fractionally quantized Hall state with anisotropic longitudinal transport. *Nat. Phys.* **7**, 845–848 (2011).
- J. P. Eisenstein, R. Willett, H. L. Stormer, D. C. Tsui, A. C. Gossard, J. H. English, Collapse of the even-denominator fractional quantum hall effect in tilted fields. *Phys. Rev. Lett.* **61**, 997–1000 (1988).
- Y. Liu, S. Hasdemir, M. Shayegan, L. N. Pfeiffer, K. W. West, K. W. Baldwin, Evidence for a  $\nu = 5/2$  fractional quantum Hall nematic state in parallel magnetic fields. *Phys. Rev. B* **88**, 035307 (2013).
- U. Wurstbauer, K. W. West, L. N. Pfeiffer, A. Pinczuk, Resonant inelastic light scattering investigation of low-lying gapped excitations in the quantum fluid at  $\nu = 5/2$ . *Phys. Rev. Lett.* **110**, 026801 (2013).
- U. Wurstbauer, A. L. Levy, A. Pinczuk, K. W. West, L. N. Pfeiffer, M. J. Manfra, G. C. Gardner, J. D. Watson, Gapped excitations of unconventional fractional quantum Hall effect states in the second Landau level. *Phys. Rev. B* **92**, 241407 (2015).
- A. L. Levy, U. Wurstbauer, Y. Y. Kuznetsova, A. Pinczuk, L. N. Pfeiffer, K. W. West, M. J. Manfra, G. C. Gardner, J. D. Watson, Optical emission spectroscopy study of competing phases of electrons in the second Landau level. *Phys. Rev. Lett.* **116**, 016801 (2016).
- G. Moore, N. Read, Nonabelions in the fractional quantum hall effect. *Nucl. Phys. B* **360**, 362–396 (1991).
- R. H. Morf, Transition from quantum hall to compressible states in the second Landau level: New Light on the  $\nu = 5/2$  enigma. *Phys. Rev. Lett.* **80**, 1505–1508 (1998).
- A. Stern, Non-Abelian states of matter. *Nature* **464**, 187–193 (2010).
- C. Nayak, S. H. Simon, A. Stern, M. Freedman, S. Das Sarma, Non-Abelian anyons and topological quantum computation. *Rev. Mod. Phys.* **80**, 1083–1159 (2008).
- K. Musaelian, R. Joynt, Broken rotation symmetry in the fractional quantum Hall system. *J. Phys. Cond. Matter* **8**, L105–L110 (1996).
- L. Balents, Spatially ordered fractional quantum Hall states. *Europhys. Lett.* **33**, 291–296 (1996).
- E. H. Rezayi, F. D. M. Haldane, Incompressible paired hall state, stripe order, and the composite fermion liquid phase in half-filled Landau levels. *Phys. Rev. Lett.* **84**, 4685–4688 (2000).
- B. Friess, V. Umansky, L. Tiemann, K. von Klitzing, J. H. Smet, Probing the Microscopic Structure of the Stripe Phase at Filling Factor  $5/2$ . *Phys. Rev. Lett.* **113**, 076803 (2014).
- T. Ando, A. B. Fowler, F. Stern, Electronic properties of two-dimensional systems. *Rev. Mod. Phys.* **54**, 437–672 (1982).
- A. Pinczuk, J. P. Valladares, D. Heiman, A. C. Gossard, J. H. English, C. W. Tu, L. Pfeiffer, K. West, Observation of roton density of states in two-dimensional Landau-level excitations. *Phys. Rev. Lett.* **61**, 2701–2704 (1988).
- C. Kallin, B. I. Halperin, Excitations from a filled Landau level in the two-dimensional electron gas. *Phys. Rev. B* **30**, 5655–5668 (1984).
- R. Shuker, R. W. Gammon, Raman-scattering selection-rule breaking and the density of states in amorphous materials. *Phys. Rev. Lett.* **25**, 222–225 (1970).

### Acknowledgments

**Funding:** The work at Columbia University was supported by the National Science Foundation, Division of Materials Research under award DMR-1306976. The Alexander von Humboldt Foundation partially supported the experimental work at Columbia University. The Molecular Beam Epitaxy (MBE) growth and transport characterization at Princeton was supported by the Gordon and Betty Moore Foundation through the EPIQS initiative grant GBMF4420 and by the National Science Foundation MRSEC grant DMR 1420541. The MBE growth and transport measurements at Purdue University are supported by the U.S. Department of Energy, Office of Basic Energy Sciences, Division of Materials Sciences and Engineering under award DE-SC0006671. **Author contributions:** U.W. performed experiments. L.D., U.W., and A.P. analyzed the data. K.W.W., L.N.P., S.F., G.C.G., and M.J.M. grew the samples. L.D. and A.P. wrote the manuscript. All authors commented on the manuscript during the writing process. **Competing interests:** The authors declare that they have no competing interests. **Data and materials availability:** All data needed to evaluate the conclusions in the paper are present in the paper and/or the Supplementary Materials. Additional data related to this paper may be requested from the authors.

Submitted 6 September 2018

Accepted 4 February 2019

Published 22 March 2019

10.1126/sciadv.aav3407

**Citation:** L. Du, U. Wurstbauer, K. W. West, L. N. Pfeiffer, S. Fallahi, G. C. Gardner, M. J. Manfra, A. Pinczuk, Observation of new plasmons in the fractional quantum Hall effect: Interplay of topological and nematic orders. *Sci. Adv.* **5**, eaav3407 (2019).